XI International Conference on Computational Plasticity. Fundamentals and Applications
COMPLAS XI
E. Oñate, D.R.J. Owen, D. Peric and B. Suárez (Eds)

NUMERICAL IMPLEMENTATION OF AN ELASTOPLASTIC MODEL FOR UNSATURATED SOILS

NUBIA A. GONZALEZ* AND ANTONIO GENS*

* Department of Geotechnical Engineering and Geosciences
Universitat Politècnica de Catalunya
Jordi Girona 1-3, Edifici D-2, 08034 Barcelona, Spain
e-mail: Nubia.Aurora.Gonzalez@upc.edu, antonio.gens@upc.edu web page: http://www.upc.edu

Key words: Unsaturated soils, constitutive model, integration algorithm, elastoplasticity, stress variables.

Abstract. This paper describes some issues related to the numerical implementation of a constitutive model for unsaturated soils based on the BBM [1]. The focus of the paper is on the stress variables used and on the numerical algorithms adopted. Conventional stress variable approach (net stress and suction) as well as the approach that takes into account the degree of saturation (Bishop's stress and suction) are examined. To solve the constitutive stress–strain equations, two stress integration procedures have been implemented, an explicit stress integration scheme with automatic substepping and error control techniques [2] and a fully implicit stress integration scheme based on the Backward-Euler algorithm with substepping [3]. Their performances during the integration of the constitutive laws are compared.

1 INTRODUCTION

There is agreement that at least two constitutive variables are generally required to represent adequately the full range of unsaturated soil behaviour, that is, including strength and deformation. Several review articles on the subject are available [4-6]. Conventional constitutive stress variable, namely net stress ($\bar{\sigma}_{ij} = \sigma_{ij} - u_a \delta_{ij}$) as well as the constitutive stress variable that takes into account the degree of saturation, commonly called Bishop's stress or average stress ($\sigma'_{ij} = \sigma_{ij} - u_a \delta_{ij} + S_r (u_a - u_w) \delta_{ij}$) are examined in this paper. In both formulations the second constitutive variable is the suction (s=u_a-u_w). σ_{ij} are total stresses, u_a the air pressure, u_w the water pressure and δ_{ij} the Kroneckers's delta. The selection of net stress or Bishop's stress or other alternative as the constitutive variable remains at present a matter of convenience [6].

Incremental stress-strain equations for unsaturated soils can be solved by a wide range of explicit and implicit integration algorithms. Explicit algorithms, use the gradients of the yield surface and plastic potential at the start of the strain increment, and their accuracy can only be controlled by breaking up the strain increment into sub-increments, special automatic

substepping and error control techniques have been proposed [2,7]. In implicit algorithms, all gradients are estimated at an advanced stress state (which is unknown) and then the resulting non-linear constitutive equations are solved by iteration [3,8]. The relative performance of implicit and explicit methods is strongly dependent on the precise form of the constitutive model. For unsaturated constitutive models, the problem of the non-convexity of the yield surface at the transition between saturated and unsaturated states can significantly complicate the implementation of these models into finite element codes [2,4]. In this paper both stress integration procedures are evaluated.

2 INTEGRATION ALGORITHMS

2.1 General

Integration algorithms will be applied to the elastoplastic BBM model for unsaturated soils [1] defined in terms of either net stresses or Bishop's stresses. In this model, suction is an additional independent variable. The constitutive equations that characterize the elasto-plastic material can be written in this particular case as:

$$\begin{aligned} &\mathrm{d}\boldsymbol{\varepsilon} = \mathrm{d}\boldsymbol{\varepsilon}^{e} + \mathrm{d}\boldsymbol{\varepsilon}^{p} + \mathrm{d}\boldsymbol{\varepsilon}^{e,s} \\ &\mathrm{d}\boldsymbol{\sigma} = \mathbf{D}^{\mathrm{e}}\left(\mathrm{d}\boldsymbol{\varepsilon} - \mathrm{d}\boldsymbol{\varepsilon}^{p} - \mathrm{d}\boldsymbol{\varepsilon}^{e,s}\right) \\ &\mathrm{d}\boldsymbol{\varepsilon}^{p} = \mathrm{d}\lambda \frac{\partial G(\boldsymbol{\sigma},k,s)}{\partial \boldsymbol{\sigma}} = \mathrm{d}\lambda \mathbf{m} \\ &\mathrm{d}k = \mathrm{d}P_o = \frac{\partial P_o}{\partial \boldsymbol{\varepsilon}^{\mathrm{p}}}\mathrm{d}\boldsymbol{\varepsilon}^{\mathrm{p}} \end{aligned} \tag{1}$$

where, $\mathrm{d}\boldsymbol{\varepsilon}$, $\mathrm{d}\boldsymbol{\varepsilon}^{e}$ and $\mathrm{d}\boldsymbol{\varepsilon}^{p}$ are increments of the total, elastic and plastic strain tensors respectively and $\mathrm{d}\boldsymbol{\varepsilon}^{e,s}$ is the contribution of suction to increment of elastic strain tensor (only necessary in the net stress formulation). **m** is the flow vector, $\mathrm{d}k$ represents the increment of hardening parameters (in this case P_0) and $\mathrm{d}\lambda$ is the plastic multiplier. Note that in above equations, $\boldsymbol{\sigma}$ vector can be either net stress ($\bar{\boldsymbol{\sigma}}$) or Bishop's stress ($\boldsymbol{\sigma}'$).

Satisfying the consistency condition,

$$\mathrm{d}F = \left(\frac{\partial F}{\partial \boldsymbol{\sigma}}\right)^{\mathrm{T}} \mathrm{d}\sigma + \frac{\partial F}{\partial s}\mathrm{d}s + \frac{\partial F}{\partial k}\mathrm{d}k = 0 \tag{2}$$

gives

$$\mathrm{d}\lambda = \frac{\mathbf{n}^{\mathrm{T}}\mathbf{D}^{e}\mathrm{d}\boldsymbol{\varepsilon} + \left(\mathrm{n}_s - \mathbf{n}^{\mathrm{T}}\mathbf{D}^{e}\mathbf{b}\right)\mathrm{d}s}{H + \mathbf{n}^{\mathrm{T}}\mathbf{D}^{e}\mathbf{m}} \tag{3}$$

$$\mathbf{n} = \frac{\partial F}{\partial \boldsymbol{\sigma}};\ \mathrm{n}_s = \frac{\partial F}{\partial s};\ \mathbf{m} = \frac{\partial G}{\partial \boldsymbol{\sigma}};\ \mathbf{b} = \frac{1}{3K_s}\boldsymbol{\delta};\ H = -\frac{\partial \mathrm{F}}{\partial P_o}\frac{\partial P_o}{\partial \varepsilon_v^{p}}\delta^{T}\mathbf{m};\ \boldsymbol{\delta}^{\mathrm{T}} = \{1,1,1,0,0,0\}$$

Note that for Bishop's stress formulation vector **b**=0. Combining equations (1) and (3), the constitutive equation integration is expressed as,

$$\begin{aligned} &\mathrm{d}\boldsymbol{\sigma} = \mathbf{D}^{\mathrm{ep}}\mathrm{d}\boldsymbol{\varepsilon} + \mathbf{W}^{\mathrm{ep}}\mathrm{d}s \\ &\mathrm{d}k = \mathbf{R}^{\mathrm{ep}}\mathrm{d}\boldsymbol{\varepsilon} + Q\mathrm{d}s \end{aligned} \tag{4}$$

where

$$\mathbf{D}^{ep} = \mathbf{D}^{e} - \frac{\mathbf{D}^{e}\mathbf{m}\mathbf{n}^{T}\mathbf{D}^{e}}{\mathrm{H} + \mathbf{n}^{T}\mathbf{D}^{e}\mathbf{m}} \quad \mathbf{W}^{ep} = -\frac{\mathbf{D}^{e}\mathbf{m}\left(\mathrm{n}_{s} - \mathbf{n}^{T}\mathbf{D}^{e}\mathbf{b}\right)}{\mathrm{H} + \mathbf{n}^{T}\mathbf{D}^{e}\mathbf{m}}$$
$$\mathbf{R}^{ep} = B\frac{\mathbf{n}^{T}\mathbf{D}^{e}}{\mathrm{H} + \mathbf{n}^{T}\mathbf{D}^{e}\mathbf{m}} \quad B = \frac{\partial P_{o}}{\partial \varepsilon_{v}^{p}}\delta^{T}\mathbf{m} \quad \mathrm{Q} = \frac{B\left(\mathrm{n}_{s} - \mathbf{n}^{T}\mathbf{D}^{e}\mathbf{b}\right)}{\mathrm{H} + \mathbf{n}^{T}\mathbf{D}^{e}\mathbf{m}} \tag{5}$$

In the integration the infinitesimal increments in the above equations (denoted by "d") are approximated with finite increments (denoted by "Δ").

2.2 Explicit algorithm

The more refined versions of the explicit algorithms [2,7] combine sub-stepping techniques with automatic sub-stepping control, error control and yield surface drift correction. An algorithm of this type has been implementedl. In this algorithm suction variable is treated as an additional strain component and it is assumed that it may be subincremented at the same rate as the other strain components.

The substepping procedure automatically divides the increment of strain and suction into a number of substeps small enough to ensure that the desired integration accuracy is enforced. The scheme involves splitting the elasto-plastic strain step $(1-\alpha)\Delta\boldsymbol{\varepsilon}$ and suction step $(1-\alpha)\Delta s$ into a series of smaller substeps, ${}^{s}\Delta\boldsymbol{\varepsilon} = \Delta T_{n}(1-\alpha)\Delta\boldsymbol{\varepsilon}$ and ${}^{s}\Delta s = \Delta T_{n}(1-\alpha)\Delta s$ (where $0 < \Delta T_{n} \le 1$), and using a modified Euler approximation for each substep. $(1-\alpha)\Delta\boldsymbol{\varepsilon}$ and $(1-\alpha)\Delta s$ are the portions of the strain increment and suction increment, respectively, that are outside of the yield surface. The size of each substep is determined by estimating the error in the stress changes and comparing it to a user-defined tolerance, *STOL*. The procedure begins assuming that only one substep is necessary. Consequently ΔT_{n} is set to unity and T_{n} is set to zero.

A first estimation of the changes in stresses and hardening parameters at the end of the pseudo-time step ΔT_{n} are evaluated using a first order Euler approximation, as,

$$\begin{aligned}\Delta\boldsymbol{\sigma}_{1} &= \mathbf{D}^{ep}\left(\boldsymbol{\sigma},k\right){}^{s}\Delta\boldsymbol{\varepsilon} + \mathbf{W}^{ep}\left(\boldsymbol{\sigma},k,s\right){}^{s}\Delta s\\ \Delta k_{1} &= \mathbf{R}^{ep}\left(\boldsymbol{\sigma},k\right){}^{s}\Delta\boldsymbol{\varepsilon} + \mathrm{Q}\left(\boldsymbol{\sigma},k,s\right){}^{s}\Delta s\end{aligned} \tag{6}$$

where, $\mathbf{D}^{ep}, \mathbf{W}^{ep}, \mathbf{R}^{ep}$ and Q are computed using equations (5). Using the above quantities, the stresses and hardening parameters at the end of the substep are $\boldsymbol{\sigma} + \Delta\boldsymbol{\sigma}_{1}$ and $k + \Delta k_{1}$, respectively. These are then used to calculate a second estimate of the changes in stress and hardening parameters over the substep, namely,

$$\begin{aligned}\Delta\boldsymbol{\sigma}_{2} &= \mathbf{D}^{ep}\left(\boldsymbol{\sigma} + \Delta\boldsymbol{\sigma}_{1}, k + \Delta k_{1}\right){}^{s}\Delta\boldsymbol{\varepsilon} + \mathbf{W}^{ep}\left(\boldsymbol{\sigma} + \Delta\boldsymbol{\sigma}_{1}, s + {}^{s}\Delta s, k + \Delta k_{1}\right){}^{s}\Delta s\\ \Delta k_{2} &= \mathbf{R}^{ep}\left(\boldsymbol{\sigma} + \Delta\boldsymbol{\sigma}_{1}, k + \Delta k_{1}\right){}^{s}\Delta\boldsymbol{\varepsilon} + \mathrm{Q}\left(\boldsymbol{\sigma} + \Delta\boldsymbol{\sigma}_{1}, s + {}^{s}\Delta s, k + \Delta k_{1}\right){}^{s}\Delta s\end{aligned} \tag{7}$$

A more accurate estimate and the end of interval ΔT_{n} is founded using the modified Euler procedure,

$$\begin{aligned}\boldsymbol{\sigma} &= \boldsymbol{\sigma} + \tfrac{1}{2}\left(\Delta\boldsymbol{\sigma}_{1} + \Delta\boldsymbol{\sigma}_{2}\right)\\ k &= k + \tfrac{1}{2}\left(\Delta k_{1} + \Delta k_{2}\right)\end{aligned} \tag{8}$$

A relative error measure is computed as,

$$R_n = \frac{1}{2}\text{máx}\left\{\frac{\left\|\Delta\boldsymbol{\sigma}_2 - \Delta\boldsymbol{\sigma}_1\right\|}{\left\|\boldsymbol{\sigma}\right\|}, \frac{\left|\Delta k_2 - \Delta k_1\right|}{k}\right\} \tag{9}$$

The current strain subincrement is accepted if R_n is not greater than *STOL*. If R_n>*STOL* then the solution is rejected and a smaller step size is computed. After accepting or rejecting the current substep, the size of the next substep is calculated based on the estimated error and the set tolerance. The next pseudo-time step is found from the relation, $\Delta T_{n+1} = q\Delta T_n$ where q is chosen so that, $R_{n+1} \le STOL$. A conservative choice for q is, $q = 0.9\sqrt{STOL / R_n}$ and it is also constrained to lie within the limits, $0.1 \le q \le 1.1$, so that, $0.1\Delta T_{n-1} \le \Delta T_n \le 1.1\Delta T_{n-1}$. The end of the integration procedure is reached when the entire increment of strain and suction is applied so that $\sum \Delta T_n = T_n = 1$.

After a successful substep the yield surface consistency condition is verified. If it is violated a drift correction procedure [9] is activated, which must ensure that the current state lies on the yield surface with a certain tolerance (*YTOL*). This correction changes both stress and internal variables but keeps the strain and suction increments unchanged.

2.3 Implicit algorithm

A fully implicit stress integration scheme based on the Backward-Euler (BE) algorithm with substepping [3] extended to unsaturated soil has been implemented. Integrating the constitutive equations with the BE methods, leads to an incremental algebraic format which is followed by a plastic corrector of the elastic trial stress violating the current yield surface. In this algorithm the plastic multiplier calculation is integrated with the internal variables updates and the incremental stress-strain relationship in a monolithic fashion.

Time-integration equation with BE scheme yields the following non-linear local problem of the type **R**=0:

$$\mathbf{R}\left\{\boldsymbol{\sigma}, k, \Delta\lambda\right\}^{(n+1)} = \begin{cases} \boldsymbol{\sigma}^{(n+1)} + \Delta\lambda\mathbf{D}^{e}\mathbf{m}^{(n+1)} - \boldsymbol{\sigma}^{(n)} - \mathbf{D}^{e\,s}\Delta\boldsymbol{\varepsilon} + \mathbf{D}^{e}\Delta\boldsymbol{\varepsilon}^{e,s} = 0 \\ k^{(n+1)} - \left(\dfrac{\partial k}{\partial \boldsymbol{\varepsilon}^{p}}\right)^{(n+1)} \boldsymbol{\delta}^{T}\mathbf{m}^{(n+1)}\Delta\lambda - k^{(n)} = 0 \\ F\left(\boldsymbol{\sigma}^{(n+1)}, k^{(n+1)}, s^{(n+1)}\right) = 0 \end{cases} \tag{10}$$

The unknowns of this local problem are the stresses $\boldsymbol{\sigma}^{(n+1)}$ and the hardening parameters $k^{(n+1)}$ at time $t^{(n+1)}$, and the plastic multiplier $\Delta\lambda$. $\Delta\boldsymbol{\varepsilon}^{e,s}$ is required only for net stress formulation and is a known variable. As in the explicit algorithm, the elasto-plastic strain step and suction step will be subdivided in smaller steps, as, ${}^{s}\Delta\boldsymbol{\varepsilon} = \Delta T_n(1-\alpha)\Delta\boldsymbol{\varepsilon}$ and ${}^{s}\Delta s = \Delta T_n(1-\alpha)\Delta s$ (where $0 < \Delta T_n \le 1$), in case that no convergence is reached in the iterative process of residual minimisation.

The non-linear system of equation (10) is solved by linearizing the residual and expanding it into a Taylor series, obtaining the following expression,

$$\mathbf{0} = \mathbf{R}\left\{\boldsymbol{\sigma}, k, \Delta\lambda\right\} + \frac{\partial\mathbf{R}\left\{\boldsymbol{\sigma}, k, \Delta\lambda\right\}}{\partial\left(\boldsymbol{\sigma}, k, \Delta\lambda\right)}\begin{bmatrix}\delta\boldsymbol{\sigma} \\ \delta k \\ \delta\lambda\end{bmatrix} + O\left[\delta^2\right] \tag{11}$$

The gradient expression $\partial_{(\boldsymbol{\sigma},k,\Delta\lambda)}\mathbf{R}\{\boldsymbol{\sigma},k,\Delta\lambda\}$ is the Jacobian matrix **J** (12). Truncating after

the first order terms, O[δ^2], and solving the linearized system of equations the new iterative update of the eight variables is obtained, as in (13)

$$\mathbf{J}\{\boldsymbol{\sigma},k,\Delta\lambda\}^{(n+1)}=\left\{\begin{array}{ccc}\mathbf{I}_{n\sigma}+\Delta\lambda\mathbf{D}^{\mathrm{e}}\dfrac{\partial\mathbf{m}}{\partial\boldsymbol{\sigma}} & \Delta\lambda\mathbf{D}^{\mathrm{e}}\dfrac{\partial\mathbf{m}}{\partial k} & \mathbf{D}^{\mathrm{e}}\mathbf{m}\\ -\Delta\lambda\dfrac{\partial k}{\partial\boldsymbol{\varepsilon}^{\mathrm{p}}}\dfrac{\partial\mathbf{m}}{\partial\boldsymbol{\sigma}} & 1-\Delta\lambda\dfrac{\partial k}{\partial\boldsymbol{\varepsilon}^{\mathrm{p}}}\dfrac{\partial\mathbf{m}}{\partial k} & -\dfrac{\partial k}{\partial\boldsymbol{\varepsilon}^{\mathrm{p}}}\mathbf{m}\\ \mathbf{n}^{T} & \dfrac{\partial F}{\partial k} & 0\end{array}\right\}_{t=t^{(n+1)}} \tag{12}$$

$$\begin{bmatrix}\delta\boldsymbol{\sigma}^{(n+1)}\\ \delta k^{(n+1)}\\ \delta\lambda^{(n+1)}\end{bmatrix}=-\left[\mathbf{J}\left\{\boldsymbol{\sigma}^{(n+1)},k^{(n+1)},\Delta\lambda^{(n+1)}\right\}\right]^{-1}\mathbf{R}\left\{\boldsymbol{\sigma}^{(n+1)},k^{(n+1)},\Delta\lambda^{(n+1)}\right\} \tag{13}$$

Adding the iterative corrector to the old values of the independent variables yields the eight updates:

$$\begin{bmatrix}\boldsymbol{\sigma}^{(n+1)}\\ k^{(n+1)}\\ \Delta\lambda^{(n+1)}\end{bmatrix}=\begin{bmatrix}\boldsymbol{\sigma}^{(n+1)}\\ k^{(n+1)}\\ \Delta\lambda^{(n+1)}\end{bmatrix}+\begin{bmatrix}\delta\boldsymbol{\sigma}^{(n+1)}\\ \delta k^{(n+1)}\\ \delta\lambda^{(n+1)}\end{bmatrix} \tag{14}$$

In some cases, when large strain increments are prescribed, the minimization of residual equations (11) is not possible after a given number of iterations. In this case, the strain and suction increments are reduced by $\Delta T_n = q\Delta T_n$, where q is chosen as 0.5. The end of the integration procedure is reached when the entire increment of strain and suction is applied so that $\sum\Delta T_n = T_n = 1$.

In order to start the iteration process, the elastic solution at the contact point with the yield surface is chosen:

$$\begin{aligned}&\boldsymbol{\sigma}_0^{(n+1)}=\boldsymbol{\sigma}^{(n)}+(1-\alpha)\mathbf{D}^{\mathrm{e}}\Delta\boldsymbol{\varepsilon}\quad;\quad k_0^{(n+1)}=k^{(n)}\\ &s_0^{(n+1)}=s^{(n)}+(1-\alpha)\Delta s\quad;\quad\Delta\lambda_0=0\end{aligned} \tag{15}$$

To solve the global problem with quadratic convergence it is necessary to use a consistent tangent matrix,

$$\frac{\partial^{n+1}\boldsymbol{\sigma}}{\partial^{n+1}\Delta\boldsymbol{\varepsilon}}=\mathbf{P}^{T}\left(\mathbf{J}^{n+1}\right)^{-1}\mathbf{P}\mathbf{D}^{\mathrm{e}} \tag{16}$$

$\mathbf{P}^{T}=(\mathbf{I}_{n\sigma}\,0\,0)$ is the projection matrix on stress space.

3 APPLICATION AND PERFORMANCE

The triaxial test on compacted Barcelona clayey silt presented in **Error! Reference source not found.** [10] was selected to examine the performance of the integration algorithms. The tests includes different types of stress paths typically performed on unsaturated soils: A1-A2, loading at constant suction, A2-A3, wetting path at constant net stress, A3-A4 drying path at constant net stress, A4-A4 shear to failure under constant suction.

Performance of numerical integration algorithms (explicit and implicit) is evaluated in terms of CPU time and the number of sub-increments required in each scheme. In all runs the yield surface tolerance is fixed at YTOL = 10^{-8}; this parameters is also used to control the

convergence of the residual in the implicit algorithm. Control error tolerance of explicit algorithm varies from STOL=10^{-2} to 10^{-6}. All CPU times presented are for an Intel Core Duo (2GHz) with 2GB of RAM. Results are presented in bar graphs where average values of the variables evaluated were computed for each stress path.

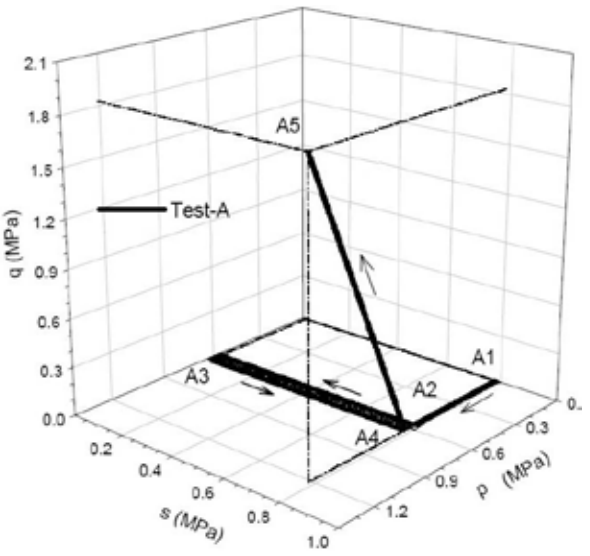

Figure 1: Stress paths followed by the test used in the evaluation of integration algorithms

Figure 2 shows a comparison between implicit and explicit algorithms for net stress and Bishop's stress. It is observed that the wetting path (A2-A3) requires both a higher computational cost and higher mean number of sub-increments when Bishop's stress and the implicit scheme are employed. This is because Bishop's stress induces a high curvature in this particular stress path. As a consequence, the plastic corrector of implicit scheme has difficulties in returning to the yield surface and the requirement for sub-increments increases. Explicit algorithm is more efficient in this case because proceeds in an incremental fashion where all gradients are estimated at known stress states. Also, it is noted for path A2-A3 that the computational cost of net stress formulation is considerably lower than that of Bishop's stress and differences between implicit and explicit schemes are minimised. Figure 2 also indicates that during stress path A1-A2 of isotropic load at constant suction, no significant differences are observed between implicit and explicit schemes. During drying path A3-A4, behaviour is elastic and no strain sub-incrementation is needed. Finally, during shearing path A4-A5, the explicit scheme demands a higher number of sub-increments than the implicit one. However, this tendency is not reflected in the CPU time, as the explicit scheme spends slightly less CPU time than implicit one. This may be explained by the fact that the implicit scheme requires second derivatives of yield function and plastic potential and the inversion of the Jacobian matrix.

Figure 3 shows the influence of the error control tolerance (*STOL*) on mean number of sub-increments and drift corrections of the explicit algorithm. As expected, the number of sub-increments and drift corrections increases as *STOL* is decreased. Due to the fact that the stress

error controls the strain sub-increments in proportion to the square root of *STOL*, their number increases by a factor of roughly $\sqrt{10}$ if *STOL* is reduced by an order of magnitude.

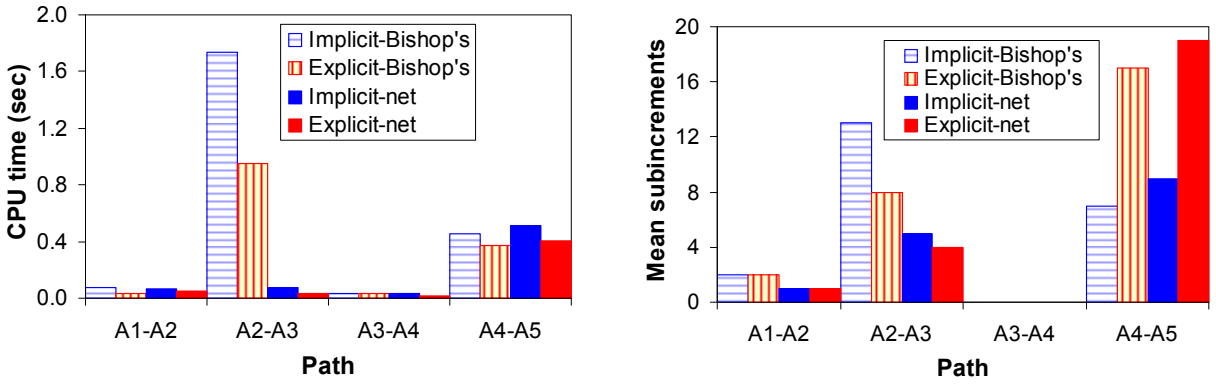

Figure 2: Comparison of integration algorithms (STOL=10^{-4} for explicit scheme)

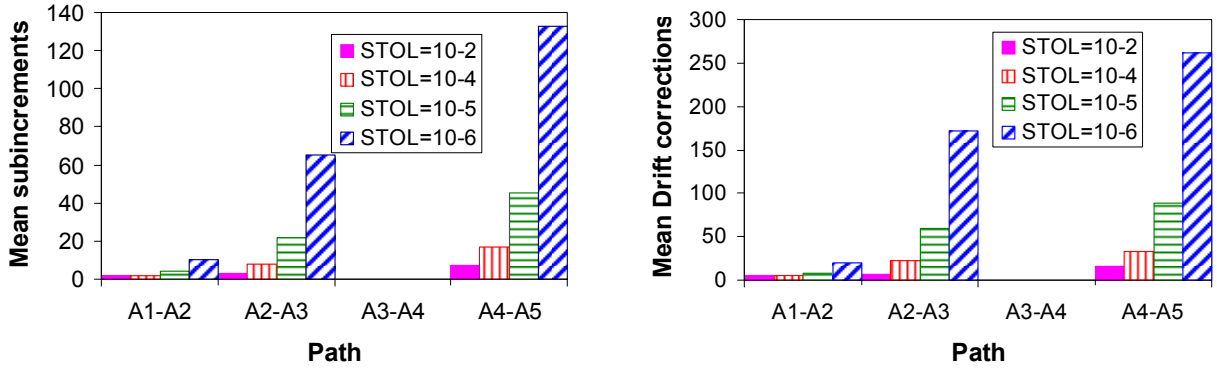

Figure 3: Influence of *STOL* on sub-increments and drift corrections of explicit algorithm. Constituive model

4 CONCLUSIONS

- Net stress is a more simple and practical choice in terms of stress path representation than Bishop's stress. However, it requires additional assumptions to take into account the shear strength increase with suction and the elastic volumetric strain due to changes in suction. Using Bishop's stresses this features derive directly from the definition of the constitutive stress. However, the performance of the model using Bishop's stress is more sensitive to the adopted soil water characteristic curve.
- In terms of the efficiency of numerical algorithms, the explicit scheme is likely to be more robust than implicit scheme to solve the kind of complex stress involved in unsaturated soil behaviour. The use of explicit scheme, however, does not yield quadratic convergence of the full problem.

ACKNOWLEDGEMENTS

The work reported has been partially funded by the European through project TUNCONSTRUCT. The support of the Spanish Ministry of Science and Innovation trough

grant BIA 2008-06537 is also gratefully acknowledged.

REFERENCES

[1] Alonso E, Gens A. and Josa A. A constitutive model for partially saturated soils. *Géotechnique* (1990) **40**:405-430.

[2] Sheng D., Sloan S.W., Gens A. and Smith D.W. Finite element formulation and algorithms for unsaturated soils. Part I: Theory. Part II: Verification and application. *Int. J. Numer. Anal. Methods Geomech.* (2003) **27**:745-790.

[3] Pérez A., Rodríguez A. and Huerta A. Consistent tangent matrices for substepping schemes. *Comput. Methods Appl. Mech. Engrg*. (2001) **190**:4627–4647.

[4] Sheng D., Gens A., Fredlund D.G. and Sloan S.W. Unsaturated soils: From constitutive modeling to numerical algorithms. *Computers and Geotechnics* (2008) **35**:810-824.

[5] Nuth M. and Laloui L. Effective stress concept in unsaturated soils: Clarification and validation of a unified framework. *Int. J. Numer. Anal. Geomech*. (2008) **32**:771-801.

[6] Gens A. Soil–environment interactions in geotechnical engineering. *Géotechnique* (2010) **60**:3–74.

[7] Sloan S.W., Abbo A.J. and Sheng D. Refined explicit integration of elasto-plastic models with automatic error control. *Engineering Computations* (2001) **18**:121–154.

[8] Vaunat J., Cante J.C., Ledesma A. and Gens A. A stress point algorithm for an elastoplastic model in unsaturated soils. *Int. J. Plasticity* (2000) **16**:121–141.

[9] Potts D. and Gens A. A critical assessment of methods of correcting for drift from the yield surface in elastoplastic finite element analysis. *Int. J. Numer. Anal. Methods Geomech*., (1985) **9**:149-159.

[10] Barrera M., Romero E., Sánchez M. and Lloret A. Laboratory tests to validate and determine parameters of an elastoplastic model for unsaturated soils. *Int. Symp. on identification and determination of soil and rock parameters for geotechnical design*. (J.P. Magna, ed.) 351-358 (2002).